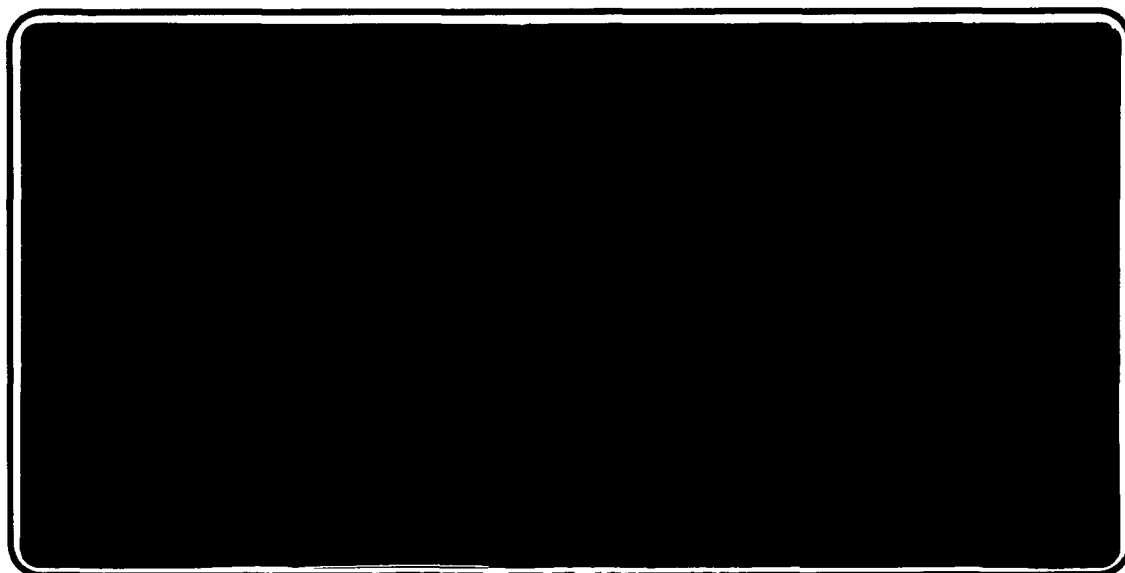Institute of Paper Science and Technology
Atlanta, Georgia

IPST TECHNICAL PAPER SERIES

NUMBER 382

Z-DIRECTIONAL PORE VOLUME DISTRIBUTION OF PIGMENT FILMS

D.T. BUNKER AND T.E. CONNERS

JUNE, 1991

Z-Directional Pore Volume Distribution of Pigment Films

D.T. Bunker and T.E. Conners

Submitted for
CPPA

Z-DIRECTIONAL PORE VOLUME DISTRIBUTION OF PIGMENT FILMS

DANIEL T. BUNKER
Ph.D. CANDIDATE
INSTITUTE OF PAPER SCIENCE AND TECHNOLOGY
ATLANTA, GA 30318

TERRANCE E. CONNERS, Ph.D.
ASSISTANT PROFESSOR OF MATERIAL SCIENCE
INSTITUTE OF PAPER SCIENCE AND TECHNOLOGY
ATLANTA, GA 30318

ABSTRACT

Transmission electron microscopy and image analysis were used to quantify the distribution of pore volume through the thickness of coating films. Clay coatings applied to nonporous media dried at high rates were found to have 2% greater pore volume than those dried at a significantly lower rate. Coatings dried at higher rates were found to be denser near the surface and bulkier through the center.

INTRODUCTION

In the last 15 years, science has made considerable strides toward understanding the art of coating technology. Recently, emphasis has been placed on how components of the coating system interact to affect product quality. For example, it has been demonstrated that coater geometry affects the fluid properties within the coater (1). Coating structure has been found to influence print density uniformity in the finished product (2,3). Drying rate or drying strategy has been shown to affect coated sheet properties (4-8). The list goes on; however, little work has been done to determine how process variables influence pigment packing and to what extent the packing structure may affect the coating properties.

The importance of the particle packing structure at the surface of the coating has been shown to be important to the microgloss of the coating (9). Smoothness and uniform density are required for even ink transfer during contact printing. The packing density of the coating is also important to its optical properties; pore size distributions have been shown to correlate with scattering coefficients (10). However, little is known about how the packing structure relates to coating strength or how the packing structure changes through the thickness of the coating; even less is known about how the density distribution is affected by the substrate or the process variables. This study is directed toward developing a laboratory technique for quantifying the pore volume distribution through the thickness of a coating layer with emphasis on the effect of drying rate on the distribution.

MATERIALS AND METHODS

Delaminated Georgia kaolin clay was dispersed in distilled water (adjusted to pH 8 with 0.1 $\underline{M}$ NaOH) to 60% solids. No dispersant was added to the clay beyond that in the clay as shipped. The Brookfield viscosities of the coatings were about 0.3 Pa·s (300 cP) at 100 rpm.

Coatings were applied to a plastic substrate using Bird bars (0.004" and 0.01" clearances) and a #10 Meyer rod. Coat weights obtained from the three metering devices were approximately 50, 100, and 20 g/m^2, respectively.

Temperature was used to control the drying rate. The rate of drying was determined by measuring the time that elapsed between when the coating was applied and when the wet-like appearance of the surface disappeared [the first critical concentration, or FCC (11)].

The solids concentration at the FCC was determined by measuring the moisture content of scrapings obtained from the coating as it reached its gloss transition point. The 60% solids delaminated clay coatings were found to reach the FCC at 77% solids.

Identical coatings were dried in an oven under slight vacuum at room temperature and at 120°C. A bright light was mounted in the back of the oven so that the gloss point could be observed easily. Coatings dried at 120°C reached the FCC after 17 ± 4 seconds. The same weight coating dried at 21°C reached the FCC after 230 ± 17 seconds, corresponding to drying rates of 1.54 kg/m^{2}hr and 0.12 kg/m^{2}hr, respectively.

Triangular samples, 7 mm at the base and 10 mm in height, were cut from the center of the coated plastic sheet for cross sectioning. A large rectangular sample was also cut from the sheet adjacent to the triangles to be used for oil absorption analysis (12). Finally, twenty 1-by-2-cm pieces were cut from each coating to be used for mercury porosimetry tests.

The triangular samples were embedded with an ultralow-viscosity resin. Thin cross sections of the embedded samples were cut with a diamond knife. Sections were collected on single-hole nickel grids according to the technique described by Abad (13).

Photomicrographs were taken at various magnifications with a transmission electron microscope (TEM). Pore volume distributions of the coating cross sections were determined from the photomicrographs using image analysis. The methods are described below.

Pore Volume Measurements

The technique used to measure the pore volume distribution through the coating thickness was similar to that used by Climpson and Taylor (10) and that of Andersson (14,15). Thin cross sections of the coating were photographed at high magnification and the resultant micrographs were analyzed using image analysis.

Digitized images (512 x 512 pixels) of coating cross sections were obtained from the photomicrographs via a video camera and frame grabber housed with the image analysis system. Each pixel was assigned a grayscale value between 0 (black) and 255 (white). Particles and pores in the digitized images were distinguished by their gray value. Figure 1 shows a photomicrograph of a coating cross section.
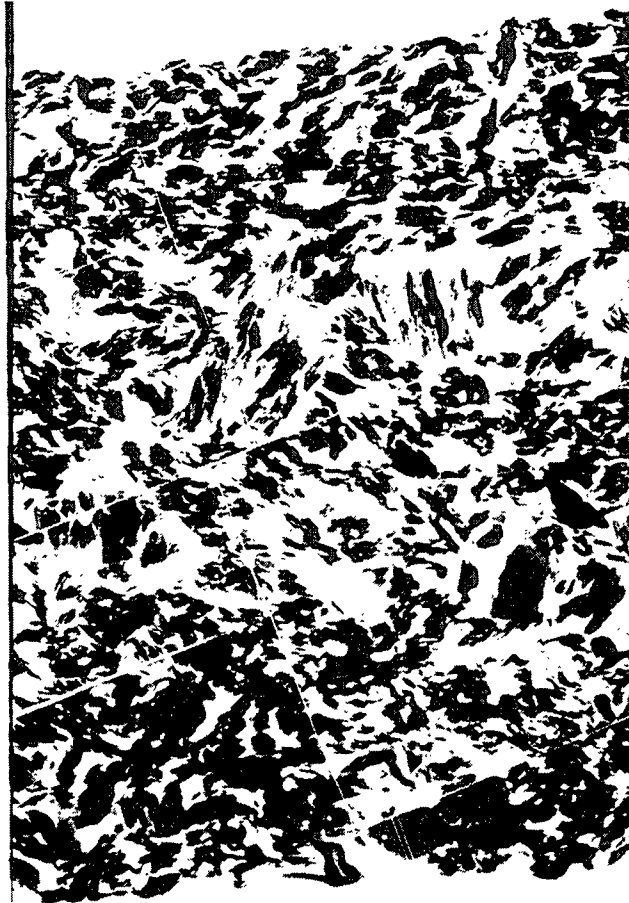
Figure 1. Composite photomicrograph of a coating cross section. 14,000x.

A binary image of the cross section is created by shifting the grayscale values. Grayscale values for pixels that make up the pigment were shifted to 0, while the grayscale values for the pores were shifted to 255. Figures 2 and 3 show a digitized image of a portion of a coating cross section and its corresponding binary.

Figure 2. Photograph of a digitized image of a cross section of a coating (enlarged).

Figure 3. Photograph of the binary image created from the grayscale image shown in Figure 2.

Applying basic stereological principles (16), the total pore volume of a cross section was determined from the binary image by taking the ratio of the number of pixels representing pores and the total number of pixels in the cross section. Density distributions were obtained by dividing the cross sections into 1-micron-thick levels and measuring the relative pore volume of each level. The value of the relative pore volume for each level was plotted against its corresponding position in the cross section. The resultant curve was used as a measure of the pore volume distribution through the coating thickness.

EVALUATION OF PORE VOLUME TECHNIQUE

Effect of Section Thickness

The thickness of a thin section of the coating cross section is critical to the resolution of the analysis method. Because both the pigment structure and the thin section are three dimensional, the section must be as thin as or thinner than the smallest pores in the coating. A section that is too thick

may have more than one layer of particles in it. When photographed, a pore lying on top of a particle will look as though it were a particle, blinding the pore to the analysis and biasing the results. Verification of this theory is shown in Figure 4.

The data in Figure 4 were obtained from a coating whose total pore volume was 42% (oil absorption), of which 95% was contained in pores greater than 0.1 micrometer in size (mercury porosimetry). Sections greater than 100 nm showed significantly lower pore volumes than the thinner sections. The accuracy of the techniques discussed in the previous section deteriorates when the section thickness approaches the size of the voids.
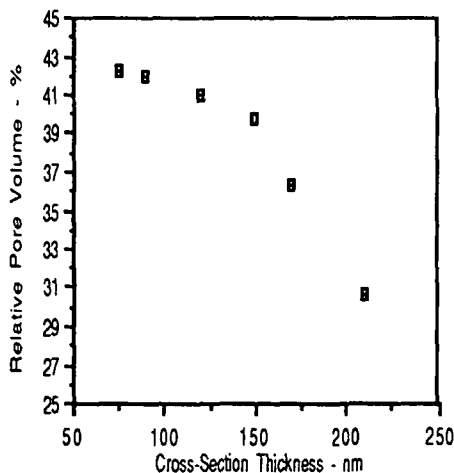

Figure 4. Relative pore volume of a 20 g/m^2 100% delaminated clay coating on a plastic film as measured by image analysis of cross-sections of various thickness.

Effect of Sample Magnification

The magnification of the sample is also important. When digitizing the image, there is some imprecision at the particle edges. Instead of a clean transition from the gray shade of the particle to that of the pore space, there is a gradual change. Due to the fuzziness at the particle edges, it is difficult to choose the grayscale value at which to divide the particles and the pores. At lower magnifications, fuzzy regions may contain a significant portion of both the pores and the particles. An error in choosing the dividing grayscale value could result in a significant error in the analysis. At higher magnification, the width of the fuzzy region becomes insignificant relative to the total number of pixels in either the pores or particles. Errors in choosing the dividing grayscale value result in insignificant changes in the analysis. Figure 5 shows the deterioration of the resolution of the analysis method below 5000x.
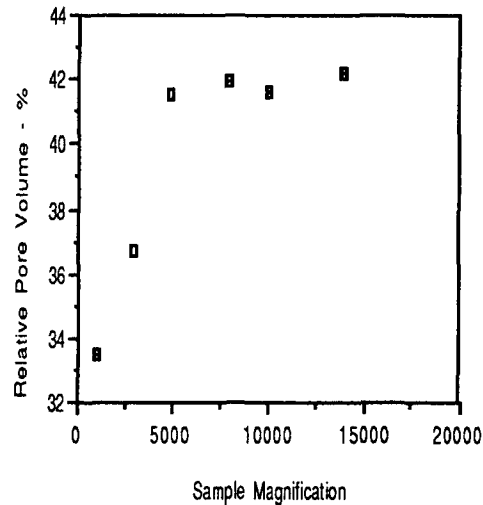
Figure 5. Relative pore volume of a coating layer versus micrograph magnification.

High magnification has its disadvantages, however. At high magnifications, the intensity of the electron beam is concentrated into a smaller area on the sample, and the absorbed energy may cause an increase in temperature or destruction of the thin section. In addition, the portion of the sample that is captured in a micrograph gets smaller with increased magnification. Because more micrographs are necessary to record a single cross section at higher magnifications, the time consumed in the analysis is increased. However, the gain in resolution by using higher magnifications outweighs the cost of the analysis time and sample preparation.

Effect of Sampling Size

A set of micrographs comprising a cross section of a coating film at 14,000x may include about 30 μm of sample length. Obviously, a single sample randomly taken from a coating will not necessarily be representative of the entire coating. From a single coating containing 40% voids, 16 separate samples were taken from random locations. Cross sections were cut parallel to the y-axis and micrographed. (The x-axis is the direction of coating application; the y-axis is perpendicular to the application direction, and the z-axis passes through the thickness of the coating.) The relative pore volumes of the samples were determined by the image analysis technique. The variance of the sample population was calculated from every combination of two or more samples. The results are shown in Figure 6. It appears that eight or more samples are necessary to obtain a representative sampling.
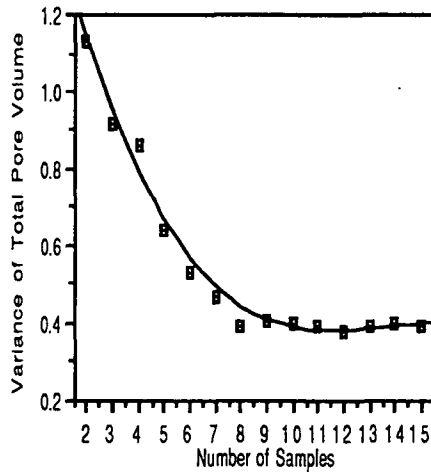
Figure 6. Relationship of the variance in total relative pore volume and the number of different samples analyzed from a single coating.

To determine if there were any specific orientations of the pores in the x-y plane, two additional sets of eight samples were cut from the same coating sample used to obtain the data in Figure 6. One set was sectioned parallel to the x-axis and the other was sectioned at 45° to the x-axis. No significant difference in total pore volume or pore volume distribution was found among the three sets of samples.

Comparison to Other Techniques

Oil absorption techniques (12) and mercury porosimetry (17) have been employed to determine the relative pore volume of each of the coatings analyzed in this study. Neither method reveals any information about the distribution of pore volume through the thickness, but each has been used to determine the total pore volume of a sample. A comparison of results of using these methods with two different coatings is shown in Figure 7.
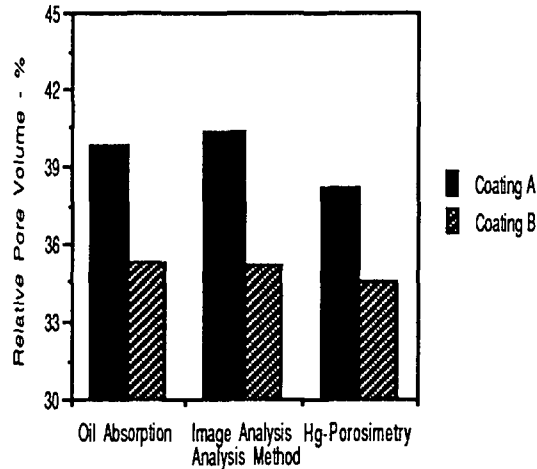
Figure 7. Total pore volume of two different coatings as determined by oil absorption, image analysis, and mercury porosimetry.

In every case tested thus far, the oil absorption method and the image analysis method have given the same results. The mercury porosimeter method was found to be significantly different at the 95% level but not at a 90% confidence level. In general, mercury porosimetry results showed about 2% less relative pore volume than the other methods. Its sample-to-sample standard deviation (1.6) was also greater than the other techniques. Data from Climpson and Taylor's (10) work indicate similar results.

INFLUENCE OF DRYING RATE: RESULTS AND DISCUSSION

Although the study of the effect of process variables on the density distribution is far from complete, the drying rate tests performed have yielded some interesting results. The drying rates obtained by oven drying (1.54 kg/m^{2}hr and 0.12 kg/m^{2}hr) are not those of industrial processes; however, the rates differed from one another by about an order of magnitude. It was expected that such extremes would produce differences in the coating structure.

The pore volume distributions through the coating thickness are shown in Figure 8. Both curves have the same general shape: dense area at approximately 2 micrometers from the surface followed by a region of high bulk which trails off near the coating base to a density similar to that of the surface.
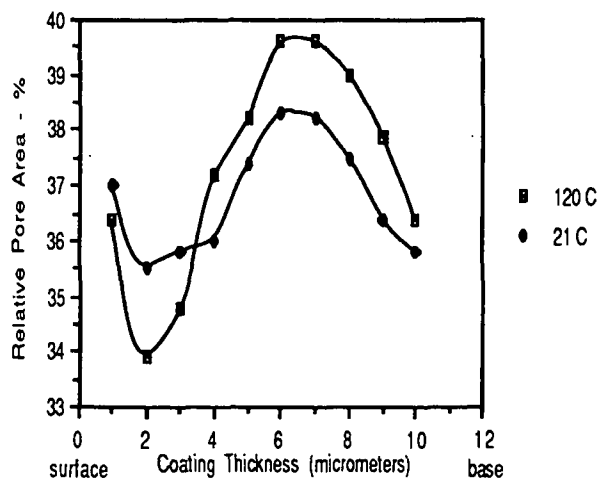
Figure 8. The z-directional pore volume distribution of 20 g/m^2 coatings dried at two different temperatures, 21° and 120°C.

The shape of the curves in Figure 8 can be explained if the colloidal interactions of the particles are considered. Hoy (18) and Hiltner and Krieger (19) have shown that particles along a boundary form regular packing structures that are denser than those of a random packed system. Particles in suspension generally are surrounded on all sides by other particles. As the particles undergo translational and rotational diffusion, they interact with neighboring particles. Each particle reacts to reduce the energy of the interaction. To achieve minimum energy, the particles at the interface orient so that a large face is parallel to the surface or so that the largest possible surface does not have a neighbor. Assuming that the clay dispersion is random and is not, for example, a "card house" structure (20), electric double-layer interactions between the surface particles and the particles below them will result in a significant parallel particle orientation. This phenomenon was observed by Climpson and Taylor (10) and by Smart (21), who studied packings of soils under compression. The parallel orientation gradually fades with depth into the dispersion. Random dispersion of uniform spheres has been reported to be restored after about 10 particle diameters (18).

Figure 8 shows that the maximum density is just below the surface instead of at the surface. The explanation lies in the measurement technique. The boundary for the coating surface was created by drawing a line between the high points on the surface. As a result, some air space above the coating is considered part of the coating, causing an apparent drop in density. The steepness of the initial drop is probably a good indication of the micro-roughness.

The bulk of the coating, 4 to 8 μm from the surface, shows the much higher bulk associated with more random structures, as would be created by out-of-plane orientation of the particles. The photomicrograph in Figure 1 shows this characteristic clearly. The substrate also acts as a boundary that

restricts movement of the interface particles. A density profile similar to that at the surface is expected. However, the density profile will probably not be as great, since the particles adhere to the substrate as coating is applied. As a result, the orientation of the interface particles may not be as uniform as it was at the surface.

The average total pore volumes of the two coatings were 37.8% ± 0.4 and 36.6% ± 0.3 for the high and low temperatures, respectively. Again, from properties of colloidal suspensions, an explanation for the difference in volume can be given. The reaction of the particles to interparticle forces is time dependent. The rate of particle orientation is the function of the orienting pressure (double-layer repulsion and surface tension forces) and the translational and rotational diffusion rate of the particles. In the system where the coating is dried quickly, the consolidation occurs too fast for some particles to react to electric double-layer forces. As a result, there is a smaller amount of parallel or structured packing and, thus, a greater void volume. This is indicated by the shallower depth of dense regions near the surfaces relative to the particles dried at a slower rate.

By the same arguments, the density near the surface of the coating should be less for the coating dried at the higher rate. However, the opposite was found. Other coatings dried at high rates have shown that the particles near the surface have a smaller size distribution than similar coatings dried at lower rates. Unpublished work by Eklund has found a similar response for calcium carbonate coatings. Capillary transport may cause water to carry small particles with it to the coating surface. However, there was no evidence that this occurred in these coatings.

Alternatively, the high drying temperature may have caused a large temperature gradient in the coating layer near the surface during drying. Because higher temperatures increase the rate of translational and rotational diffusion and lower the viscosity of the dispersing media, higher temperatures favor ordered packing. A large temperature gradient near the surface could result in denser packing near the surface compared to coatings dried at lower temperatures.

CONCLUSIONS

The image analysis method provides reliable results for quantification of pore volume distribution through the thickness of a coating film. The accuracy of the distribution is critically dependent upon the thickness of the cross sections; resolution is lost when section thickness is larger than the smallest significant fraction of the pores. The method is also dependent upon the sample magnification; a too-low magnification may result in deterioration of the accuracy of the analysis.

Coatings were found to vary in density from surface to substrate. The density variation can be explained by interaction of colloidal particles near boundaries.

Coatings dried at widely different temperatures and water removal rates were found to have similar density distributions. Higher temperatures resulted in greater total pore volume and denser, but shallower, regions near the coating surface. The greater pore volume resulted from a more random structure caused by limiting the time available for the particles to respond to interparticle

and boundary interactions. It is not readily apparent what caused the increased density near the coating surface.

Further indepth investigations into drying rate effects are in progress. Coatings are being dried at constant temperature, and drying rates are being controlled by changing the humidity of drying air blown over the surface of the coating. Similar experiments are being performed on coatings made of polystyrene latex. Study of particles of easily modeled geometry may lead to a better understanding of the roles played by colloidal and hydrodynamic forces in the coating layer during drying.

ACKNOWLEDGMENT

LITERATURE   CITED

1. TRIANTAFILLOPOULOS, N. G. Fluid Dynamics of Short-Dwell Blade Coater Ponds and Their Relationship to Cross Directional Coat Weight Nonuniformities. Ph.D. Thesis (Institute of Paper Science and Technology). 1990.

2. BAUMEISTER, M.; KRAFT, K. Quality Optimization by Control of Coating Structure. Tappi Journal 64(1): 85-89 (Jan. 1981).

3. MISHIBA, S.; UCHIDA, A.; ISHIKAWA, T.; TAKAHASHI, K. Observation of Binder Migration by Electron Microscope. Tappi Coating Conference (Cincinnati) Proceedings pp. 79-85 (May 21-23, 1979).

4. ENGSTROM, G.; FINEMAN, I.; PERSSON, A.; KARLSSON, I.; AKESSON, R. Experiences with Drying of Starch Containing Coating Colors in Air Float Dryers. Wochenbl. Papierfabr. 108(19):793-799 (Oct. 15, 1980).

5. ENGSTROM, G.; FINEMAN, I.; PERSSON, A.; AKESSON, R. How Drying Conditions Influence Ink-Mottling in Offset Printing. Tappi Journal 65(11):81-84 (Nov. 1982).

6. LINDSTROM, Y.; PALSANEN, J. Influence of Air Drying on the Quality of Offset Paper. Wochenbl. Papierfabr. 111(14):491-495 (July 31, 1983).

7. STEPHANSEN, E. W. New High-Intensity Infrared Radiation Reduces Binder Migration on Coating. Tappi Journal 69(2):42-44 (Feb. 1986).

8. ENGSTROM, G.; NORRDAHL, P.; STROM, G. Studies of the Drying and Its Effect on Binder Migration and Offset Mottling. Tappi Coating Conference (Houston) Proceedings pp. 35-43 (May 17-21, 1987).

9. KENT, H. J.; CLIMPSON, N. A.; COGGON, L.; HOOPER, J. J.; GANE, P. A. C. Novel Techniques for Quantitative Characterization of Coating Structure. Tappi Journal 69(5):78-83 (May 1986).

10. CLIMPSON, N. A.; TAYLOR, J. H. Pore Size Distributions and Optical Scattering Coefficients of Clay Structures. Tappi Coating Conference (Boston) Proceedings. pp. 85-94 (May 17-19, 1976).

11. WATANABE, J.; LEPOUTRE, P. A Mechanism for the Consolidation of the Structure of Clay-Latex Coatings. Journal of Applied Polymer Science. 27:4207-4219 (1982).

12. LEPOUTRE, P; REZANOWICH, A. Optical Properties and Structure of Clay-Latex Coatings. Tappi Journal. 60(11):86-91 (Nov. 1977).

13. ABAD, A. A Study of Section Wrinkling on Single Hole Coated Grids Using TEM and SEM. Journal of Electron Microscopy Technique. 8(3):217-222 (1988).

14. ANDERSSON, H. Image Analysis in Paper Research at STFI. Proc. Third Scandinavian Conf. Image Analysis. (Johansen, P. and Becker, P. W. eds.), Studentlitteratur, Lund, Sweden, pp. 194-198 (1983). Original not seen. Cited by Bristow and Kolseth (15).

15. BRISTOW, J. A.; KOLSETH, P. Paper: Structures and Properties. New York: Marcel Dekker, Inc. pp. 162-167 (1986).

16. WEIBEL, E. R. Stereological Methods. vol. 1. London: Academic Press. pp. 9-60 (1979).

17. GAREY, C. L.; LEEKLEY R. M.; HULTMAN, J. D.; NAGEL, S. C. Determination of Pore Size Distribution of Pigment Coatings. Tappi Journal 56(11):134-138.

18. HOY, K. L. The Effect of Particle-Size Distribution on the Rheology and Film Formation of Latex Coatings. in Organic Coatings (Parfitt, G. D. and Patsis, A. V. eds.). New York: Marcel Dekker, Inc. vol. 5:123-146 (1983).

19. HILTNER, P. A.; KRIEGER, I. M. Diffraction of Light by Ordered Suspensions. The Journal of Physical Chemistry. 73(7):2386-2389 (July 1969).

20. VAN OLPHEN, H. An Introduction to Clay Colloid Chemistry. New York: John Wiley & Sons. 2nd ed. pp. 92-108 (1977).

21. SMART, P. Particle Arrangements in Kaolin. in Clays and Clay Minerals vol. 15. pp. 241-254 (1967).